Reaction $^{36}Ar(p,\gamma)^{37}K$ in explosive hydrogen burning

C. Iliadis, J. G. Ross, J. Görres, and M. Wiescher
University of Notre Dame, Notre Dame, Indiana 46556

S. M. Graff
Los Alamos National Laboratory, Los Alamos, New Mexico 87545

R. E. Azuma
University of Toronto, Toronto, Ontario, Canada M5S 1A7

(Received 10 February 1992)

The reaction $^{36}Ar(p,\gamma)^{37}K$ has been measured in the proton energy range of $E_p=0.32$–0.93 MeV. A new resonance was found at $E_R=321$ keV. We have measured the branching ratios and the resonance strength. The stellar reaction rates which are dominated by this resonance for temperatures $T=0.07$–0.9 GK are calculated. Network calculations have been performed to investigate the influence of the new stellar rates on the time evolution of the ^{36}Ar abundance during explosive H burning.

PACS number(s): 25.40.Lw, 27.30.+t, 95.30.Cq

I. INTRODUCTION

Hydrogen burning, at temperatures and densities far in excess of those attained in the interiors of ordinary main-sequence stars, may occur in various astrophysical sites, including novae, x-ray bursts, and supernova explosions. For these explosive and hydrogen-rich environments, the *rp* process has been proposed [1] as a fast nucleosynthesis reaction sequence whereby CNO material will be transferred into the Fe-Ni mass region. The resulting network of nuclear reactions involves proton and alpha capture, (p,α) reactions, and β-decay processes, as well as possible inverse reactions, and extends from the line of stability up to the proton drip line.

Recent numerical network calculations [2] indicate that the main reaction flow in the mass $A=30$–40 range will lead to the production of ^{36}Ar for typical temperatures $T=0.2$–0.6 GK and densities $\rho=10^2$–10^6 g/cm^3. Figure 1 shows the result of a calculation for a constant temperature $T=0.4$ GK and density $\rho=10^3$ g/cm^3. For the initial elemental-abundance distribution, solar isotopic abundances have been used. The dominant reaction path is given by

$$^{33}Cl(p,\gamma)^{34}Ar(\beta^+\nu)^{34}Cl(p,\gamma)^{35}Ar(p,\gamma)^{36}K(\beta^+\nu)^{36}Ar$$

with an alternative branch via

$$^{35}Ar(\beta^+\nu)^{35}Cl(p,\gamma)^{36}Ar\ .$$

Therefore, the stellar rate of the subsequent reaction $^{36}Ar(p,\gamma)^{37}K$ determines the flow towards heavier mass regions.

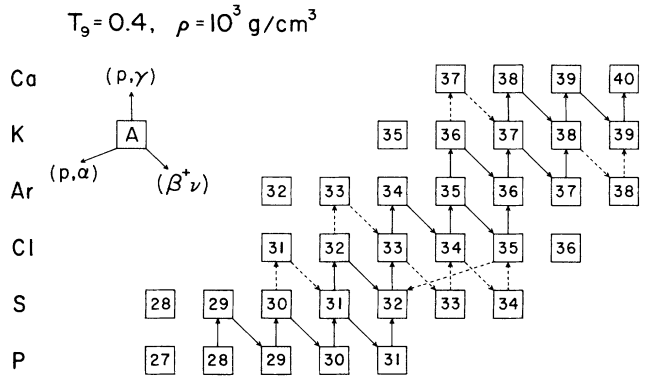

FIG. 1. Major nuclear flows in the *rp* process integrated over a period of $t=1000$ s for the $A=30$–40 mass range. The calculation was performed for a constant temperature $T=0.4$ GK and density $\rho=10^3$ g/cm^3. Solid arrows indicate dominant nuclear flows. Dashed arrows indicate flows roughly an order of magnitude weaker.

The proton capture on ^{36}Ar was previously investigated by Goosman and Kavanagh [3] and by de Esch and van der Leun [4] in the bombarding energy range $E_p>0.9$ MeV. Figure 2 shows the level diagram of ^{37}K with the corresponding resonances in the $^{36}Ar+p$ channel and the important energy windows for different stellar temperatures. The lowest-lying resonance has been observed [3] at $E_R=917$ keV. The reaction rates for $^{36}Ar(p,\gamma)^{37}K$ have been previously estimated by Wallace and Woosley [1] considering this resonance only. However, for temperatures of interest here ($T<1$ GK), the Gamow windows are located well below this proton energy. In fact, there are two more states known [3,4] between the proton threshold and the resonance at $E_R=917$ keV. The corresponding resonance energies are $E_R=321$ and 440 keV, respectively. We therefore investigated the reaction $^{36}Ar(p,\gamma)^{37}K$ in the astrophysically important energy range $E_p=300$–920 keV.

Throughout this work, E_p is the proton bombarding energy and E_R labels the resonance energy. Both energies are given in the laboratory system unless stated otherwise.

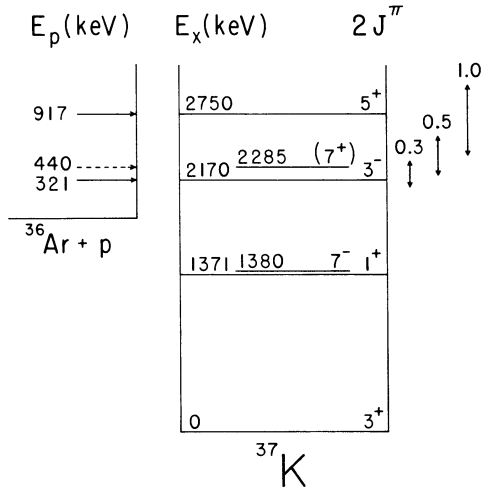

FIG. 2. Level diagram of ^{37}K and proton energies of resonances in the reaction ^{36}Ar$(p,\gamma)^{37}$K. The Gamow windows for different stellar temperatures T_9 (10^9 K) are also indicated.

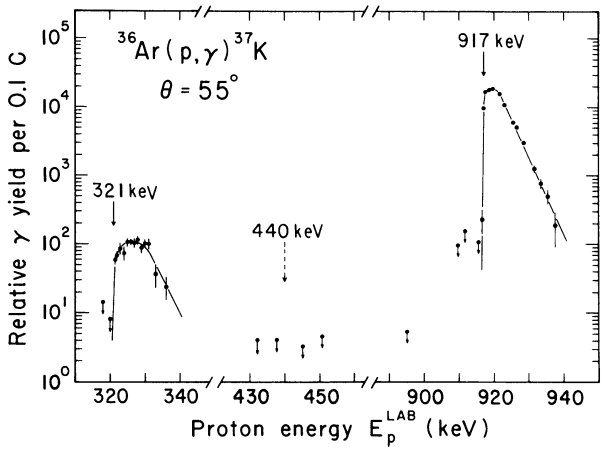

FIG. 3. Excitation function for ^{36}Ar$(p,\gamma)^{37}$K, measured at $\theta=55°$ for the primary transition to the ground state in ^{37}K. The data points shown are not corrected for the γ-ray efficiency of the Ge detector. The resonance at $E_R=321$ keV has not been observed previously. The ratio of target thicknesses at $E_p=321$ and 917 keV agrees with the corresponding ratio of the effective stopping powers. The solid line is to guide the eye.

II. APPARATUS

The 1-MV Van de Graaff accelerator at the University of Toronto supplied proton beams of up to 70 μA on target in the energy range of $E_p=0.3$–1.0 MeV, with an energy resolution of $\Delta E=1$ keV and an energy calibration better than ± 2 keV. The proton beam passed through a Ta collimator and was directed onto the target which was mounted at 45° with respect to the beam direction. A liquid-nitrogen-cooled copper tube was placed between the collimator and the target to minimize carbon deposition on the target. The target and chamber formed a Faraday cup for charge integration and a negative voltage (-300 V) was applied to the Cu tube to suppress secondary electron emission from the target.

The ^{36}Ar target was made by implanting Ar ions into a 0.5-mm-thick Ta backing with a charge density of 54 mC/cm^2 and an implantation energy of 80 keV, yielding a thickness of ≈ 7 keV at $E_p=917$-keV bombarding energy. The thick target yield curve for the $E_R=917$-keV resonance in ^{36}Ar$(p,\gamma)^{37}$K is shown in Fig. 3. The target stoichiometry was determined from the known [3] strength of this resonance, $\omega\gamma=0.208\pm0.03$ eV. Using the stopping power tables of Andersen and Ziegler [5], a ratio of tantalum to argon of $N_{\rm Ta}/N_{\rm Ar}=6.5\pm1.3$ has been obtained. The target was directly water cooled and was checked several times during the course of the experiment. No noticeable deterioration was observed over an accumulated charge of 6 C.

The γ-ray spectra was measured with a 37% Ge detector. The energy resolution was 2.0 keV at $E_\gamma=1.3$ MeV. The detector was placed at $\theta_\gamma=55°$ with respect to the beam direction at a front-face-to-target distance of $d=1.8$ cm and was shielded by 5 cm of lead to reduce room background contributions. The γ-ray efficiencies were determined using a calibrated ^{60}Co source as well as the γ rays from the resonance [6] at $E_R=992$ keV in the ^{27}Al$(p,\gamma)^{28}$Si reaction. Since the Ge detector was positioned in close geometry to the target, coincidence summing [7] of γ rays had to be considered. We have estimated the effect of coincidence summing on the absolute γ-ray efficiency at $E_\gamma=1333$ keV to be less than 9% using the calibrated ^{60}Co source strength and the intensities of the γ lines at $E_\gamma=1173$ and 1333 keV and of their summing peak. This uncertainty was included in the errors for the full-energy peak efficiency.

III. EXPERIMENTAL RESULTS AND DISCUSSION

Gamma-ray spectra were measured in the bombarding energy range $E_p=320$–930 keV with charge accumulations of 0.01–1 C. Figure 3 shows the yield curve for the primary decay to the ground state of ^{37}K. Two resonances have been observed at $E_R=917$ and 321 keV.

The resonance at $E_R=917$ keV was known from earlier work [3,4]. Our measured resonance energy and branching ratios are listed in Tables I and II, and they are in agreement with the values from the literature.

The resonance at $E_R=321$ keV had not been seen previously. Both the resonance energy and the observed primary γ energies, however, correspond within the experimental errors to the state at $E_x=2170$ keV ($J^\pi=\frac{3}{2}^-$) in the compound nucleus ^{37}K. This state was observed in transfer reaction studies [3] and in $(p,\gamma\gamma)$ work [4]. We, therefore, adopt spin and parity of $J^\pi=\frac{3}{2}^-$ for this resonance. Figure 4 shows the on-resonance γ spectrum taken at $E_p=325$ keV. In addition to the strong ground-state branching, a weak primary decay to the first excited state at $E_x=1371$ keV ($J^\pi=\frac{1}{2}^+$) is also observed (see Table II). This branch has not been seen in the earlier $(p,\gamma\gamma)$ work of Ref. [4] where the state at $E_x=2170$ keV was populated by the γ decay of higher-lying resonances.

TABLE I. Energies and strengths for $^{36}Ar(p,\gamma)^{37}K$ resonances.

E_R (keV)		J^π	$\omega\gamma$ (eV)[e]	
Present	Ref. [4]	(Ref. [4])	Experiment	Calculated[f]
321±2[a]	321.3±0.2[b]	$\frac{3}{2}^-$	$(6.1\pm1.4)\times10^{-4}$ [c]	6.3×10^{-4}
	439.5±0.2[b]	$\frac{7}{2}^+$	$\leq2.4\times10^{-5}$ [c]	$\leq2.5\times10^{-5}$
917±2[a]	917.52±0.07	$\frac{5}{2}^+$	0.208±0.030[d]	0.095

[a]From the location of midpoint of front edge of thick target yield curve.
[b]Calculated from known E_x and $Q_{p\gamma}=(1857.57\pm0.09)$ keV.
[c]From the present work; the quoted values have been obtained relative to the strength of the resonance at $E_R=917$ keV (see text).
[d]From Ref. [3]; used as a reference for the calculation of the target stoichiometry.
[e]With $\omega\gamma=(2J_R+1)\Gamma_p\Gamma_\gamma/2\Gamma$.
[f]Calculated from Eq. (1) by estimates of the partial widths Γ_γ and Γ_p (see text).

The corresponding secondary ground-state transition of the level at $E_x=1371$ keV is also indicated in Fig. 4 and agrees in intensity, after correction for the different γ-ray efficiencies, with the primary decay.

The strength $\omega\gamma$ of a (p,γ) resonance is defined by

$$\omega\gamma=\frac{2J+1}{(2j_p+1)(2j_t+1)}\frac{\Gamma_p\Gamma_\gamma}{\Gamma} \quad (1)$$

with J, j_p, and j_t as spin of the resonance, the projectile, and the target nucleus, respectively; Γ is the total width of the resonance, and Γ_p,Γ_γ are the corresponding partial widths. The resonance strength is related to the thick-target yield Y_R of a resonance [8] by

$$\omega\gamma=\frac{2\varepsilon_{\text{eff}}}{\lambda_R^2}\frac{A_t}{A_t+A_p}Y_R\ , \quad (2)$$

where λ_R is the proton wavelength at the resonance energy, A_t (A_p) the mass of the target (projectile) in u, and ε_{eff} the effective stopping power of the ArTa target compound:

$$\varepsilon_{\text{eff}}=\varepsilon_{\text{Ar}}+(N_{\text{Ta}}/N_{\text{Ar}})\varepsilon_{\text{Ta}} \quad \text{with } N_{\text{Ta}}/N_{\text{Ar}}=6.5\pm1.3\ .$$

The stopping power values for ε_{Ar} and ε_{Ta} were taken from Ref. [5]. For the newly observed resonance at $E_R=321$ keV, a value of $\omega\gamma=(6.1\pm1.4)\times10^{-4}$ eV has been obtained (see Table I). The quoted error includes the uncertainty of the effective stopping power (±20%), the relative γ-ray efficiency (±7%), and the charge measurement (±5%).

No resonance has been observed at $E_p=440$ keV, corresponding to the state at $E_x=2285$ keV ($J^\pi=\frac{7}{2}^+$). Us-

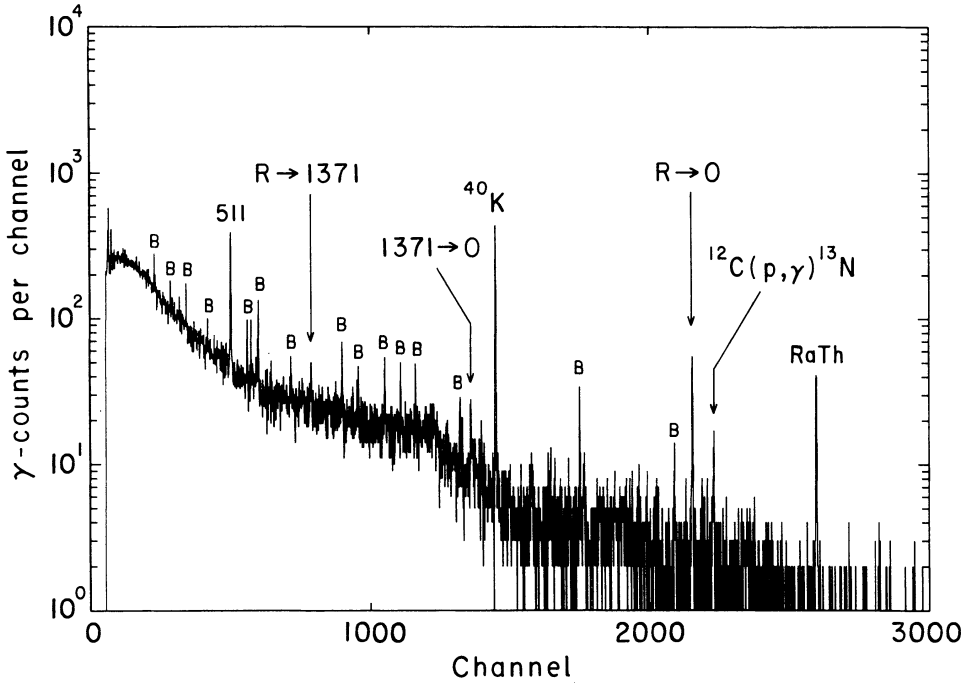

FIG. 4. On-resonance γ-ray spectrum, measured at $\theta=55°$ for the new observed resonance at $E_R=321$ keV. The γ-ray energies above peaks are in keV. Background contributions are labeled.

TABLE II. Gamma-ray branching ratios (in %) of ^{37}K states.

	E_R (keV)	321		917	
	E_{xi} (keV)	2170		2750	
E_{xf}	J^{π}[a]	$\frac{3}{2}^-$		$\frac{5}{2}^-$	
(keV)		Present	Ref. [4]	Present	Ref. [4]
0	$\frac{3}{2}^+$	87±6	100	98.6±0.9	98.2±0.1
1371	$\frac{1}{2}^+$	13±4	<4		
1380	$\frac{7}{2}^-$		<4	1.4±0.4	1.5±0.1
2170	$\frac{3}{2}^-$			<0.4	0.3±0.1

[a]From Ref. [4].

ing the known branching ratio [4] of this state, an upper limit of $\omega\gamma \leq 2.4\times10^{-5}$ eV has been determined (see Table I).

The branching ratios and $\omega\gamma$ values have been deduced from spectra taken at $\theta_\gamma = 55°$ [where $P_2(\cos\theta)=0$], assuming that any possible $P_4(\cos\theta)$ component in the angular distribution is negligible. This is clearly the case for the $J=\frac{3}{2}$ resonance at $E_R=321$ keV. Also, the measured angular distribution [4] of the resonance at $E_R=917$ keV ($J=\frac{5}{2}^+$) indicates only an A_2 component. For the possible resonance at $E_p=440$ keV ($J^\pi=\frac{7}{2}^+$), no correction for angular distribution effects has been applied in the calculation of the upper limit for $\omega\gamma$.

It is interesting to compare the measured resonance strengths with the values obtained from Eq. (1) by an estimate of the partial widths Γ_γ and Γ_p. Such calculated resonance strengths are frequently used for the derivation of stellar reaction rates if the respective values for $\omega\gamma$ cannot be measured directly. The γ partial width Γ_γ of unbound ^{37}K states can be deduced from the known lifetimes [9] of the bound mirror states in ^{37}Ar. The proton partial width Γ_p can be parametrized [8] as

$$\Gamma_p = 3\frac{\hbar^2}{\mu R^2}P_l C^2 S \ . \tag{3}$$

Here, the quantity R denotes the nuclear channel radius, μ the reduced mass, P_l the penetrability at the resonance energy E_i for the orbital angular momentum l of the resonance, and C^2 the isospin Clebsch-Gordan coefficient ($C^2=1$ for $T=\frac{1}{2}$ states). The single-particle spectroscopic factors S were adopted from Hagen *et al.* [10]. The resulting strengths of $\omega\gamma = 6.3\times10^{-4}$ and 9.5×10^{-2} eV for the resonances at $E_R=321$ and 917 keV, respectively, are in the same order of magnitude as the directly measured values (see Table I). For the assumed g-wave resonance at $E_R=440$ keV, no spectroscopic factor is known. Using the Wigner limit $C^2S=1$ results in a theoretical upper limit for the strength of $\omega\gamma \leq 2.5\times10^{-5}$ eV, similar to the experimentally obtained upper limit (see Table I).

To search for possible direct capture (DC) transitions, an off-resonance γ spectrum was taken at a proton bombarding energy of $E_p=895$ keV with a total accumulated charge of 1 C. No γ transitions to final states in ^{37}K could be observed. The cross sections that result from DC model calculations (see Sec. IV) are 2 orders of magnitude smaller than the experimentally determined upper limits of $\sigma^{DC} \leq 40$ nb.

IV. ASTROPHYSICAL IMPLICATIONS

The stellar reaction rate $N_A\langle\sigma v\rangle$ of ^{36}Ar$(p,\gamma)^{37}$K can have contributions from narrow resonances and the direct capture process into the low-lying states in ^{37}K. The reaction rate (in units of reactions $s^{-1}\,mol^{-1}\,cm^3$) for isolated narrow resonances is given by the expression [11]

$$N_A\langle\sigma v\rangle = 1.54\times10^{11}[\mu T(\mathrm{GK})]^{-3/2} \times \sum_i (\omega\gamma)_i \exp[-11.605E_i/T(\mathrm{GK})] \ , \tag{4}$$

where the reduced mass μ is an u and the strengths $\omega\gamma_i$ and c.m. energies E_i of the resonances are in MeV. For temperatures of interest here ($T<1$ GK), all resonances with $E_i<2042$ keV were considered. The E_i and $\omega\gamma_i$ values for resonances located in the energy range of the present experiment were taken from Table I. Otherwise, the values of Refs. [3,4] have been used. The reaction rate contribution for the resonances at $E_R=321$ and 917 keV are listed in columns 2 and 4 of Table III, respectively. To investigate the maximum contribution of the assumed resonance at $E_R=440$ keV, the stellar rates have been calculated with the experimentally found upper limit (see Table I). The resulting values are shown in column 3 of Table III.

For the calculation of the nonresonant reaction rates, the cross sections of the DC process for transitions to all bound states in ^{37}K were calculated using the formalism described by Rolfs [12]. The single-particle spectroscopic factors were adopted from Ref. [10]. The sum of the astrophysical S factors for all final states was parametrized below $E_p=1.5$ MeV by the polynomial

$$S(E)=0.1195-4.630\times10^{-2}E+1.4996\times10^{-2}E^2 \tag{5}$$

with S in MeV b and E the c.m. energy in MeV. The stellar reaction rates were calculated using the expressions for nonresonant reaction mechanisms [11] and are listed in column 5 of Table III.

The total reaction rates are shown in column 6 of

TABLE III. Stellar reaction rates $N_A\langle\sigma v\rangle$ of $^{36}Ar(p,\gamma)^{37}K$ in units of (cm^3/mol s).

T_9 (10^9 K)	$N_A\langle\sigma v\rangle$ 321[a]	440[b]	917[c]	DC[d]	Total[e]
0.05	2.71×10^{-28}	2.72×10^{-41}		1.46×10^{-24}	1.46×10^{-24}
0.06	3.67×10^{-23}	3.16×10^{-34}	2.34×10^{-69}	1.32×10^{-22}	1.68×10^{-22}
0.07	1.64×10^{-19}	3.39×10^{-29}	9.58×10^{-59}	4.77×10^{-21}	1.68×10^{-19}
0.1	5.44×10^{-13}	3.42×10^{-20}	1.08×10^{-39}	9.63×10^{-18}	5.44×10^{-13}
0.3	3.34×10^{-3}	1.54×10^{-6}	2.04×10^{-10}	8.35×10^{-10}	3.34×10^{-3}
0.5	1.96×10^{-1}	5.33×10^{-4}	9.48×10^{-5}	4.70×10^{-7}	1.96×10^{-1}
0.8	1.47	1.09×10^{-2}	1.11×10^{-1}		1.58
0.9	2.04	1.82×10^{-2}	3.92×10^{-1}		2.43
1.0	2.60	2.69×10^{-2}	1.06		3.66
1.5	4.74	7.67×10^{-2}	1.82×10^{1}		2.30×10^{1}
2.0	5.64	1.14×10^{-1}	6.64×10^{1}		7.35×10^{1}

[a]Contribution of new observed resonance at $E_R=321$ keV.
[b]Maximum contribution of assumed resonance at $E_R=440$ keV, calculated with the experimentally determined upper limit for $\omega\gamma$ (see Table I).
[c]Contribution of resonance at $E_R=917$ keV.
[d]Contribution of direct capture into states at $E_x=0$, 1371, and 1380 keV in ^{37}K.
[e]Total reaction rate contribution of resonances $E_R=321$–2042 keV and DC.

Table III and they are also displayed in Fig. 5 with the individual contributions discussed above. It can be seen that the new resonance at $E_R=321$ keV determines the stellar rates over the entire temperature range of $T=0.07$–0.9 GK . At very low temperatures, $T<0.07$ GK, the DC process dominates, while the resonance at $E_R=917$ keV contributes substantially only at high temperatures $T>0.9$ GK. The assumed resonance at $E_R=440$ keV and all other resonances with $E_R\geq1259$ keV, are negligible for temperatures $T<1.5$ GK.

The resonance at $E_R=321$ keV increases $N_A\langle\sigma v\rangle$ by several orders of magnitude for temperatures $T<0.9$ GK (see Table III). To investigate the impact of our new results on the expected abundance of ^{36}Ar during explosive H burning, we have performed network calculations using the new and old stellar rates, respectively. Figure 6 shows the time evolution of the ^{36}Ar abundance, obtained for a constant temperature and density ($T=0.4$ GK, $\rho=10^3$ g/cm^3) over a time period of 1000 s. The old rates predicted an appreciable enrichment by nearly 2 orders of magnitude over the initial solar abundance of ^{36}Ar. Due to its small depletion rate at this temperature, ^{36}Ar is not processed further towards heavier masses within the time scale of the calculation. The use of the new rate, however, leads to a substantially different result. The initial ^{36}Ar abundance is reduced by 3 orders of

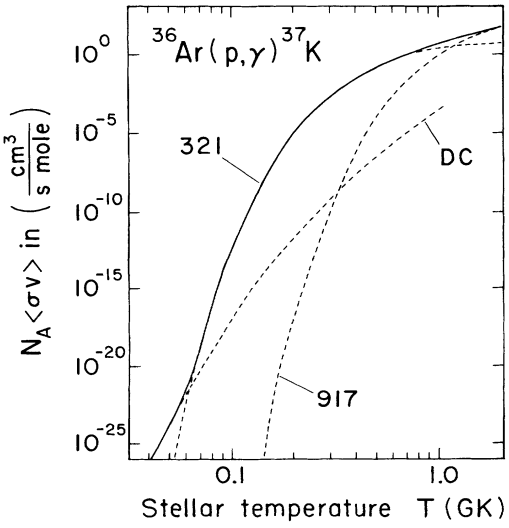

FIG. 5. Total stellar reaction rate (solid line) and individual contributions (dashed lines) for the reaction $^{36}Ar(p,\gamma)^{37}K$.

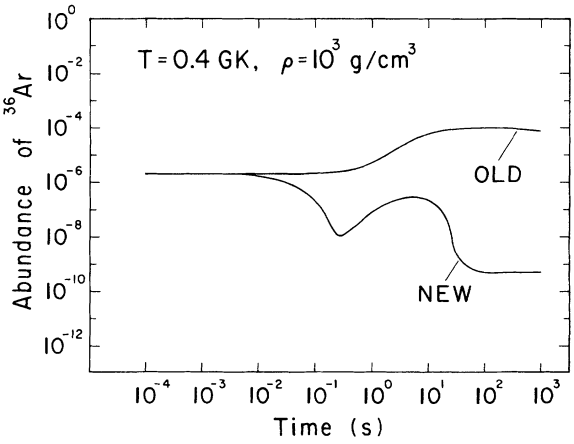

FIG. 6. Abundance of ^{36}Ar vs time for a constant temperature $T=0.4$ GK and density $\rho=10^3$ g/cm^3. The two curves shown result from using the old and new stellar rates for the reaction $^{36}Ar(p,\gamma)^{37}K$, respectively.

magnitude at the end of the calculation. The new stellar reaction rate of $^{36}Ar(p,\gamma)^{37}K$ is large enough to guarantee a strong mass flow towards heavier nuclei at temperatures $T=0.2$–0.6 GK.

This work was supported by U.S. National Science Foundation Grant No. PHY88-03035 (Notre Dame) and by the Natural Sciences and Engineering Research Council of Canada.

[1] R. K. Wallace and S. E. Woosley, Astrophys. J. Suppl. **45**, 389 (1981).
[2] L. A. van Wormer, Ph.D. thesis, University of Notre Dame, 1990 (unpublished).
[3] D. R. Goosman and R. W. Kavanagh, Phys. Rev. **161**, 1156 (1967).
[4] H. P. L. de Esch and C. van der Leun, Nucl. Phys. **A476**, 316 (1988).
[5] H. H. Andersen and J. F. Ziegler, *Stopping Powers and Ranges in All Elements* (Pergamon, New York, 1977).
[6] A. Antilla, J. Keinonen, M. Hautala, and I. Forsblom, Nucl. Instrum. Methods **147**, 501 (1977).
[7] K. Debertin and R. G. Helmer, *Gamma- and X-Ray Spectrometry with Semiconductor Detectors* (North-Holland, Amsterdam, 1988).
[8] H. E. Gove, in *Nuclear Reactions I,* edited by P. M. Endt and M. Demeur (North-Holland, New York, 1959).
[9] P. M. Endt, Nucl. Phys. **A521**, 1 (1990).
[10] M. Hagen, U. Janetzki, K.-H. Maier, and H. Fuchs, Nucl. Phys. **A152**, 404 (1970).
[11] W. A. Fowler, G. R. Caughlan, and B. A. Zimmerman, Annu. Rev. Astron. Astrophys. **23**, 69 (1975).
[12] C. Rolfs, Nucl. Phys. **A217**, 29 (1973).